Disorder-induced rounding of the phase transition in the large-q-state Potts model

M. T. Mercaldo,[1,2] J-Ch. Anglès d'Auriac,[1] and F. Iglói[3,4]

[1]*Centre de Recherches sur les Trés Basses Tempèratures, Boîte Postale 166, F-38042 Grenoble, France*

[2]*Dipartimento di Fisica "E.R. Caianiello" and Istituto Nazionale per la Fisica della Materia, Università degli Studi di Salerno, Baronissi, Salerno I-84081, Italy*

[3]*Research Institute for Solid State Physics and Optics, H-1525 Budapest, P.O. Box 49, Hungary*

[4]*Institute of Theoretical Physics, Szeged University, H-6720 Szeged, Hungary*

The phase transition in the q-state Potts model with homogeneous ferromagnetic couplings is strongly first order for large q, while it is rounded in the presence of quenched disorder. Here we study this phenomenon on different two-dimensional lattices by using the fact that the partition function of the model is dominated by a single diagram of the high-temperature expansion, which is calculated by an efficient combinatorial optimization algorithm. For a given finite sample with discrete randomness the free energy is a piecewise linear function of the temperature, which is rounded after averaging, however, the discontinuity of the internal energy at the transition point (i.e., the latent heat) stays finite even in the thermodynamic limit. For a continuous disorder, instead, the latent heat vanishes. At the phase transition point the dominant diagram percolates and the total magnetic moment is related to the size of the percolating cluster. Its fractal dimension is found $d_f = (5 + \sqrt{5})/4$ and it is independent of the type of the lattice and the form of disorder. We argue that the critical behavior is exclusively determined by disorder and the corresponding fixed point is the isotropic version of the so-called infinite randomness fixed point, which is realized in random quantum spin chains. From this mapping we conjecture the values of the critical exponents as $\beta = 2 - d_f$, $\beta_s = 1/2$, and $\nu = 1$.

I. INTRODUCTION

Quenched disorder has generally a softening effect on the singularities of phase transitions in homogeneous systems. As an example we mention that in the two-dimensional (2D) Ising model the ordered phase (and thus the phase transition) is washed out by random fields [1,2], whereas due to layered bond randomness the Onsager logarithmic singularity in the specific heat of the homogeneous system will turn into a very weak essential singularity (McCoy-Wu model) [3]. Singularities at first-order phase transitions are also softened [4]. In 3D the latent heat is either reduced by a finite extent (for weak disorder) or the latent heat completely disappears and the transition becomes second order (for sufficiently strong disorder) [5]. In 2D, according to the rigorous result by Aizenman and Wehr [1] there is no phase coexistence in the presence of continuous disorder, thus the phase transition is always continuous. Thus there exists a set of random fixed points whose possible classification is a great challenge of statistical physics. However, as in the theory of disordered systems, exact results in this field are scarce and therefore our present understanding of the subject is limited. Since a weak-disorder perturbation calculation starting from the pure system's fixed point is not feasible most of the existing results are numerical. In this respect an important role is played by the q-state ferromagnetic Potts model [6], in which the homogeneous phase transition is of first order for $q > 4$ in 2D [7] and for $q \geq 3$ in 3D.

According to Monte Carlo [8] and transfer-matrix [9] investigations the critical behavior of the 2D random bond Potts model (RBPM) is governed by a line of q-dependent fixed points. For a given q the critical exponents are expected to be disorder independent; however, generally there is a strong crossover regime [10]. The anomalous dimension of the magnetization, x, shows a smooth, monotonously increasing q dependence, which saturates at a given finite value as $q \to \infty$. On the other hand the critical exponent of the correlation length, ν, which is related to energy-density correlations, is found to show only a very weak q dependence. The measured values are all around the rigorous bound [11], $\nu = 2/d = 1$, which is required by general theorem for disordered systems. (Note, however, the conflicting result in Ref. [9], which is probably due to the use of the bimodal, i.e., discrete form of disorder.)

Despite the intensive numerical studies performed so far several aspects of the phase transition in the RBPM are not clarified yet. Here we mention that there is still little knowledge about the mechanism which leads to the softening of the first-order transition. The effect of different types of disorder, continuous or discrete, has not been investigated. Also universality of the transition with respect to the lattice structure is still an open question. Finally, and most importantly, there is no example for a specific system in which the critical properties are (conjecturedly) exactly known.

In this paper we are going to investigate the aforementioned questions using the example of the 2D RBPM in the large-q limit. The use of this model has several advantages: (i) The homogeneous model, which has a strongly first-order phase transition, can be solved analytically [6]. (ii) In the presence of randomness the model shows the generic features of disorder-rounded first-order phase transitions. (iii) It allows for an important technical simplification since the high-temperature expansion of the model [12] (with arbitrary ferromagnetic couplings) is dominated by a single diagram, whose calculation is reduced to an optimization problem [13]. (iv) Finally, this optimization problem is polynomial and there exists a powerful combinatorial optimization algorithm [14] which works in strongly polynomial time, i.e., the

necessary computational power does not depend on the actual form of the disorder.

This model, which we shall refer simply as random bond Potts model in the following, has already been considered in several previous works. Cardy and Jacobsen [9] have shown a mapping with the random-field Ising model in the level of interface Hamiltonians, which explains the vanishing of the latent heat at the transition point. Numerical studies for large (but finite) q values [15] predicted a smooth and nonsingular behavior of the critical exponents as $q \to \infty$. Relation of the random bond Potts model with an optimization problem was introduced and studied by the method of simulated annealing in Ref. [13]. The optimization problem was mathematically analyzed in Ref. [14]. Here its relation with submodular function optimization was shown and an efficient computational algorithm was developed. Some numerical results obtained by the optimization method have been briefly announced in a paper [16].

The structure of the paper is the following. The model, its random cluster representation, and the way how its thermodynamical and correlational properties are related to the dominant diagram are given in Sec. II. In Sec. III the mechanism of breaking of phase coexistence is analyzed and an estimate of the breaking-up length is given through extreme value statistics. Thermal quantities (internal energy, specific heat) are calculated in Sec. IV. In particular we study the effect of discrete and continuous disorder as well as the location of the transition point for different 2D lattices. The magnetization properties of the model, which are related to the percolative properties of the largest connected cluster of the dominant diagram, are studied in Sec. V. In Sec. VI we show arguments and approximate mappings between our model and random quantum spin chains which lead us to conjecture the exact values of the critical exponents. Our conclusions are drawn in the final section while two simple examples are given in the Appendix.

II. FORMALISM: THE LARGE-q-STATE POTTS MODEL

The q-state Potts model [6] is defined by the Hamiltonian

$$\mathcal{H} = -\sum_{\langle i,j \rangle} J_{ij} \delta(\sigma_i, \sigma_j) \tag{1}$$

in terms of the Potts-spin variables $\sigma_i = 0, 1, \ldots, q-1$ at site i. The summation runs over all edges of a lattice $\langle i,j \rangle \in E$, and in our study the couplings, $J_{ij} > 0$, are independent identically distributed (i.i.d.) random variables. We consider the system in the large-q limit where, being the entropy per site $s \sim \ln q$, it is convenient to introduce the reduced temperature $T' = T \ln q = O(1)$ and its inverse as $\beta' = 1/T' = \beta/\ln q$. In the following we use these reduced variables but omit in the notation the prime. In terms of these variables the partition function is given by

$$Z \equiv \sum_{\{\sigma\}} q^{-\beta \mathcal{H}(\{\sigma\})}, \tag{2}$$

which is convenient to express in the random cluster representation [12] as

$$Z = \sum_{G \subseteq E} q^{c(G)} \prod_{ij \in G} [q^{\beta J_{ij}} - 1]. \tag{3}$$

Here the sum runs over all subsets of bonds, $G \subseteq E$, and $c(G)$ stands for the number of connected components of G.

In the large-q limit, where $q^{\beta J_{ij}} \gg 1$, the partition function can be written as

$$Z = \sum_{G \subseteq E} q^{\phi(G)}, \quad \phi(G) = c(G) + \beta \sum_{ij \in G} J_{ij}, \tag{4}$$

which is dominated by the largest term, $\phi^* = \max_G \phi(G)$, so that

$$Z = n_0 q^{\phi^*} (1 + \cdots). \tag{5}$$

Here the degeneracy of the optimal set G^* is $n_0 = O(1)$ and the omitted corrections in the right-hand side (rhs) go to zero for large q. The free energy per site is proportional to ϕ^* and given by

$$-\beta f = \frac{\phi^*}{N}, \tag{6}$$

where N stands for the number of sites of the lattice. In the Appendix we give an illustration of the convergence with q of the family of function $f_q(\beta)$.

All information about the random bond Potts model is contained in the optimal set G^*. The thermal properties are calculated from ϕ^*, whereas the magnetization and the correlation function are obtained from its geometrical structure. First we note that correlation between two individual sites is unity only if both are in the same connected cluster, otherwise the correlation is zero. In this way the *average* correlation function $C(r)$ is related to the distribution of clusters in the optimal set. Next we note that if, and only if, there is an infinite cluster the correlation function approaches a finite asymptotic value, $\lim_{r \to \infty} C(r) = m^2$. The magnetization m, defined in this way, is the fraction of sites in the infinite cluster. In the ferromagnetic phase, $T < T_c$, the magnetization is $m > 0$ and vanishes at the critical point T_c as $m \sim (-t)^\beta$, where the relative distance from the phase transition point is measured by $t = (T - T_c)/T_c$. As usual the divergence of the correlation length ξ at the critical point is given in the form $\xi \sim |t|^{-\nu}$, where ξ is defined as the average size of the clusters. At the critical point the largest cluster is a fractal and its mass M scales with the linear size of the system L as $M \sim L^{d_f}$, where d_f is the fractal dimension. Spin-spin correlations at the critical point decay algebraically as $C(r) \sim r^{-2x}$, where the magnetization scaling dimension is given by $x = d - d_f = \beta/\nu$.

In a system with a free surface one can define surface quantities, whose singularities are governed by surface exponents. In the ferromagnetic phase the fraction of surface sites belonging to the largest cluster defines the surface magnetization, which scales as $m_s \sim (-t)^{\beta_s}$. At the critical point surface-surface correlations decay as $C_s(r) \sim r^{-2x_s}$ and the surface scaling dimension x_s is related to the surface fractal dimension d_f^s as $d - 1 = d_f^s + x_s$. We have also $\beta_s = x_s \nu$.

In the random bond Potts model in the large-q limit the structure and the fractal properties of the optimal set are dominated by disorder effects. Other examples of systems in which the disorder is dominant at the critical point are random quantum spin chains [17], for which the set of critical exponents is exactly known. This analogy and a possible isomorphism between the fixed points of the two problems, which will be discussed in detail in Sec. VI, lead us to conjecture the value of the critical exponents for the random bond Potts model, which we list below.

The fractal dimension of the infinite cluster at the transition point and the scaling dimension of the (bulk) magnetization are related to the golden-mean ratio, $\phi = (1 + \sqrt{5})/2$, as

$$d_f = 1 + \phi/2, \quad x = 1 - \phi/2. \tag{7}$$

The analogous surface quantities are conjectured to be

$$d_f^s = 1/2, \quad x_s = 1/2. \tag{8}$$

Finally, the correlation length exponent is given by

$$\nu = 1, \tag{9}$$

thus saturating the rigorous bound for disordered systems [11]: $\nu \geq 1$.

We close this section by a few technical remarks. The cost function of the problem $\phi(G)$, given in Eq. (4), is a supermodular function, thus there exists a combinatorial optimization method [18] to maximize it. For the particular expression of $\phi(G)$ in the present model a specific efficient algorithm, the optimal cooperation algorithm [14], has been formulated. The largest random system we treated by this method is a 512×512 square lattice.

The investigations in this paper are restricted to two dimensions. In particular we work on the square lattice for which the location of the critical point is known for some distribution of the couplings. For $0 < \beta J_{ij} < 1$ and for a symmetric distribution $P(\bar{J} + J) = P(\bar{J} - J)$, where $\bar{J}$ is the mean coupling, the critical point is given by self-duality as [19]

$$T_c = \frac{1}{\beta_c} = 2\bar{J}. \tag{10}$$

In the numerical calculations we used either a discrete (bimodal) distribution,

$$P_b(J) = p\,\delta(\bar{J} - \Delta - J) + (1-p)\,\delta(\bar{J} + \Delta - J), \tag{11}$$

which is symmetric for $p = 1 - p = 1/2$, or a continuous (uniform) distribution,

$$P_u(J) = \begin{cases} 1/2\Delta & \text{for} \quad \bar{J} - \Delta < J < \bar{J} + \Delta \\ 0 & \text{otherwise.} \end{cases} \tag{12}$$

In practical applications the latter distribution is approximated by a set of discrete peaks [see, for example, Eq. (19)], which is necessary since the algorithm works in terms of rational numbers. In the numerical calculations we collected data about systems up to a linear size $L = 256$. The number of realizations were about 10^6 for the smaller systems and around 10^3 for the largest one. To check universality, we

considered non-self-dual randomness, analyzing triangular and hexagonal lattices with number of sites up to 16384.

III. DESTRUCTION OF PHASE COEXISTENCE DUE TO DISORDER

In this section we consider the phase transition in the nonrandom system and see how introduction of disorder will destroy the phase coexistence, i.e., soften the first-order phase transition into a second-order one. In particular in 2D we will estimate the disorder dependent length scale l_b, at which the phase coexistence no longer exists.

The solution of the optimization problem in Eq. (5) depends on the temperature: the optimal set is generally more interconnected in low temperature and contains more disconnected parts in higher temperature. In the homogeneous, nonrandom model with $J_{ij} = J$ there are only two (trivial) homogeneous optimal sets: the fully connected diagram and the empty diagram. Consequently the free energy of the homogeneous system (f_{hom}) is given by

$$-N\beta f_{\text{hom}} = \begin{cases} 1 + N\beta Jz, & T < T_c \\ N, & T > T_c, \end{cases} \tag{13}$$

where z is the connectivity of the lattice. At the phase-transition point, $\beta_c = 1/T_c = (1 - 1/N)/(Jz)$, there is phase coexistence, thus the phase transition is of first order and the latent heat Δe has its possible maximal value: $\beta_c \Delta e = 1$. Note that this result holds for any regular (even finite) lattice.

As quenched disorder is switched on, say in the paramagnetic phase, its fluctuations will locally prefer the existence of the nonstable fully connected homogeneous diagram, and this tendency is stronger around the phase-transition point, where the free-energy difference between the two homogeneous phases is small. This mechanism, as the temperature is lowered, will result in a sequence of nonhomogeneous optimal sets with increasing fraction of connected component, whose average size is just the correlation length ξ. If ξ stays finite at the phase transition point then there is phase coexistence and thus the first-order nature of the transition persists. This is the case in 3D for sufficiently weak disorder.

In 2D, however, for any small amount of continuous disorder the correlation length is divergent at the transition point, thus the phase transition softens to second order. This is true in the thermodynamic limit, while in a finite system of linear size L weak disorder fluctuations could be not sufficient to break phase coexistence. The finite length scale, $l_b = L$, at which the breaking of phase coexistence takes place, can be estimated through extreme value statistics in the following way [20].

At the transition point of the homogeneous system, i.e., at $\beta = 1/(Jz)$, we compare the stability of the empty graph with a nonhomogeneous diagram G_S, in which all sites are isolated except that of a domain of S spins, which are fully connected. The relative cost function is given by

$$W = \beta \sum_{ij \in G_S} J_{ij} - S + 1$$

$$= \beta \sum_{ij \in G_S} (J_{ij} - J) + \beta J (Sz - \alpha S^{1/2}) - S + 1$$

$$\simeq \frac{S^{1/2}\Delta}{zJ}(\zeta - J\alpha/\Delta) + 1, \tag{14}$$

FIG. 1. Nonhomogeneous optimal diagram for the bimodal distribution at a size $L=256$, corresponding to the breaking up disorder, $\Delta/J=693/2693=0.2573$. The connected part of the diagram is compact and percolates in one direction.

where we used that the distribution is symmetric, with $\bar{J}=J$. Here in the second line the number of occupied edges of G_S is Sz minus the missing bonds at the perimeter of the fully connected domain, which is given by $\alpha S^{1/2}$. In the last equation we used that we are at the critical temperature and introduced the representation $\Sigma_{ij}(J_{ij}-J)=\Delta S^{1/2}\zeta$, in terms of the Gaussian random variable ζ, which has zero mean and variance one.

Next we consider all independent positions of the fully connected domain in the finite lattice, whose number is denoted by N_S, and look for the largest value of the cost function, W_0, in these diagrams. According to extreme value statistics [21] in the large N_S limit its value is related to the cumulative probability distribution $P(W>W_0)$ and follows from the equation

$$N_S P(W>W_0)=1. \tag{15}$$

Making use of the relation for a Gaussian variable, $P(\zeta>\zeta_0)\simeq\exp(-\zeta_0^2/2)/\zeta_0$, we obtain from Eq. (15) that $W_0>0$, i.e., the new diagram has a larger cost function than the empty set, if $N_S>\exp[\mathrm{const}(J/\Delta)^2]$. Here we are interested in the case when S is in the same order as L^2, i.e., when there is a complete breaking of the homogeneous diagram, in which case N_S scales as $N_S\sim L^a$, with $0<a<2$. Thus the breaking-up length scale is just $l_b\sim L$ and given by

$$l_b\approx l_0\exp\left[A\left(\frac{J}{\Delta}\right)^2\right], \tag{16}$$

where l_0 is a reference length.

The relation between l_b and Δ has been studied numerically, by calculating the smallest Δ at which the breaking of phase coexistence in a system of size L takes place. (We used periodic boundary conditions.) An example of a nonhomogeneous optimal diagram obtained in this way for the bimodal disorder is illustrated in Fig. 1.
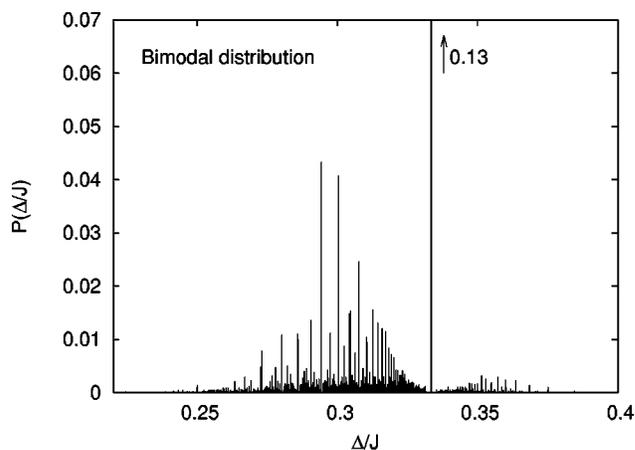

FIG. 2. Distribution of the breaking-up strength of bimodal disorder for a size $L=64$. The large individual peak at $\Delta/J=1/3$ corresponds to an instability due to a 3×3 plaquette.

For the bimodal disorder the distribution of the limiting values of Δ for a given size $L=64$ is shown in Fig. 2. The distribution consists of several individual peaks; some of those are related to instabilities due to small finite plaquettes. The size of the smallest such plaquette, l, is given by $l\sim J/\Delta$, but the typical size of a connected domain varies between l and L, thus there are strong sample-to-sample fluctuations. We have checked the validity of the relation in Eq. (16) for the bimodal distribution and the result is plotted in Fig. 3. In the region of size $L\lesssim128$ we could work the asymptotic behavior in Eq. (16) has not yet been reached; the data points deviate from the expected straight line. The effective behavior of the breaking-up length for these sizes is better described (the relative error is 0.003) by a dependence $\ln L\sim J/\Delta$, as seen in the inset. In the numerical calculation J/Δ goes to infinity faster than the prediction given above in Eq. (16), because we implicitly consider in Eq. (14) a Euclidean domain S, whereas the optimal cooperation algorithm finds more complicated domains.
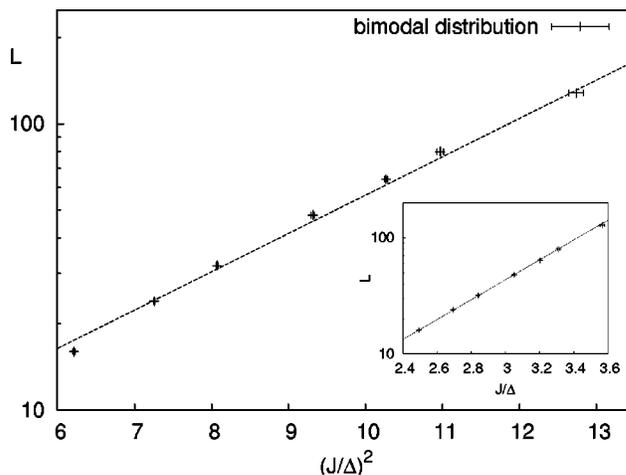

FIG. 3. System size L as a function of the inverse average breaking-up disorder, $(J/\Delta)^2$, for bimodal distribution. (In the average of J/Δ we considered the contribution of all peaks). For the sizes we considered a fit with (J/Δ) is better, as shown in the inset.
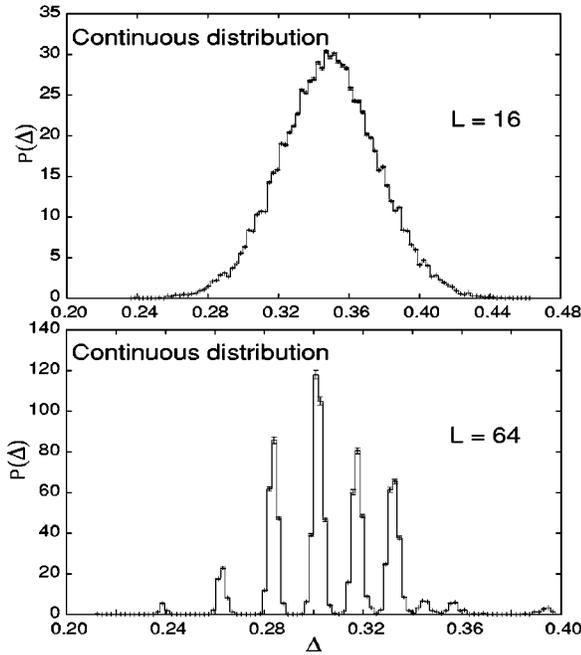
FIG. 4. Distribution of the breaking-up strength of quasicontinuous disorder composed of $m=127$ individual peaks in Eq. (19) for two different sizes. For larger sizes the separated peaks are due to the discreteness of the disorder.

We have repeated this calculation by using a (quasi)continuous disorder, which is approximated by 127 discrete peaks. As seen in Fig. 4 now the distribution of the breaking strength Δ, for a relatively small size $L=16$, is Gaussian-like; however, for a size $L \geq 32$, there is a secondary structure reflecting the effect of discreteness in the representation of disorder. As can be seen in Table I, the measured breaking strengths are consistent with the result in Eq. (16), unless for the two larger sizes, where the effect of discreteness of the distribution becomes significant.

In the numerical calculations on the critical properties of the RBPM, whose results are reported in the following sections, we always choose the disorder strong enough, so that the relation $L \gg l_b$ is satisfied.

At this point we comment on a relation between the RBPM in the large-q limit and the random-field Ising model (RFIM) at $T=0$, which has already been observed by Cardy and Jacobsen [9]. The form of the cost function in Eq. (14) is identical to that of the RFIM, where bonds in the RBPM are

TABLE I. Breaking strengths for the continuous disorder (for the fourth column $L_0 \simeq 1$ is used).

L	$\left\langle \dfrac{\Delta(L)}{J} \right\rangle$	$\sigma_{\Delta/J}$	$\left(\dfrac{\Delta}{J} \right)^2 \ln\dfrac{L}{L_0}$	Samples
16	0.34854	0.00016	0.3368	31324
24	0.3275	0.0002	0.3408	13927
32	0.3142	0.0002	0.3422	14786
48	0.3133	0.0002	0.3801	15561
64	0.3075	0.0004	0.3932	2878

equivalent to sites in the RFIM having a random field of $J_{ij}-J$ and the perimeter contribution in Eq. (14) is related to the domain-wall energy in the RFIM. Thus βJ corresponds to the ferromagnetic coupling in the RFIM. This mapping on the level of the interface Hamiltonian is, however, restricted to a smooth, nonfractal interface. Therefore it applies in the same way in the stability analysis of the pure phases, resulting in a similar breaking-up length scale as in Eq. (16). However the (fractal) structures of the clusters in the two problems are different. As a consequence the bulk and surface fractal dimensions (and the related critical exponents) are different in the two problems. For the RFIM the percolating clusters have the same fractal properties as ordinary (site) percolation, as has been demonstrated by numerical calculations [22].

IV. SINGULARITIES OF THERMAL QUANTITIES FOR DISCRETE AND CONTINUOUS DISORDER

In this section we analyze the singularities of thermal quantities, in particular we consider the internal energy e and the specific heat c_V. We start to rewrite Eq. (6) for the free energy of a given realization of disorder as

$$F = -c(G^*)T - \sum_{ij \in G^*} J_{ij}, \qquad (17)$$

where the optimal set G^* changes discontinuously as temperature is varied. For sufficiently high temperature, $\beta'z \max(J)<1$, G^* is the empty set, whereas for low temperatures, $\beta'z \min(J)>1$, it is fully connected. In between, around the transition point, however, there are more frequent changes. In a finite system of size L, the temperature interval of stability of the optimal set is found numerically to be around $\sim 1/L$ for the bimodal distribution. As a consequence in a finite system the free energy is a piecewise linear function of the temperature, whose slope [the entropy $c(G^*)$] is monotonously increasing with the temperature. From Eq. (17) the internal energy is obtained by derivation, which for a given sample is

$$E = -\sum_{ij \in G^*} J_{ij}. \qquad (18)$$

This is a piecewise constant function of the temperature. Thus in a given sample, even for a finite system, the internal energy shows discontinuities. We illustrate this point in a simple example in the Appendix, where the comparison between the bimodal and the uniform distributions for a general simple triangle is given. In the given (finite) sample the phase transition point separates the two qualitatively different regimes in which the largest cluster is not percolating (paramagnetic phase) from that in which it is percolating (ferromagnetic phase). This phase transition in the given sample is sharp and of first order. Later we shall use this definition to locate the transition point of a series of samples and study their distribution.

In the random system, as we mentioned before, the average quantities, such as the average free energy and its derivatives, are of physical relevance. The averaging procedure
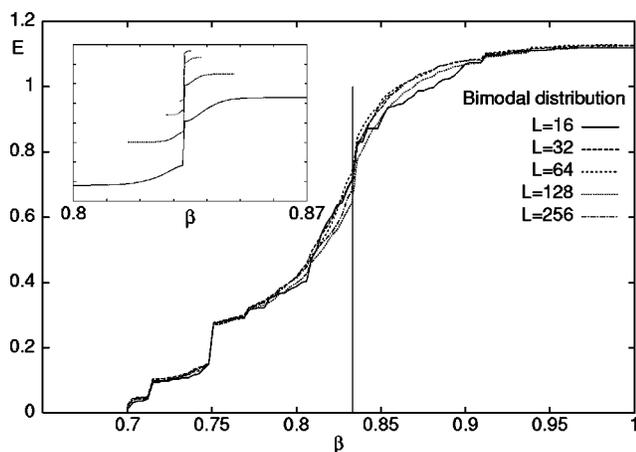
FIG. 5. Internal energy with bimodal disorder ($\beta J_1 = 1/6$ and $\beta J_2 = 5/6$) as a function of the inverse temperature β. Note the discontinuities which are present after averaging in the thermodynamic limit, cf. at $\beta = 0.75$. In the inset the discontinuous behavior at the transition point $\beta = 5/6$ is illustrated (the lines from bottom to top are for increasing size from $L=32$ to $L=256$).

generally acts to smear out the discontinuities in the internal energy. In this respect the behavior of the averaged quantities is different for the discrete and the continuous distributions. (See also the example in the Appendix.) As illustrated in Fig. 5 for the bimodal distribution several discontinuities remain in the average internal energy, whereas for the uniform distribution the average internal energy is continuous, as illustrated in Fig. 6. For the discrete distribution the origin of the discontinuities is the degeneracies of ϕ at some temperature. For example, consider a square lattice where the bonds follow the bimodal distribution in Eq. (11). In this lattice let us focus on an elementary square, whose bonds are all strong. The sites of this plaquette are either nonconnected (giving a contribution to f of $4T$) or fully connected [with a contribution to f of $T + 4(\bar{J} + \Delta)$]. These two situations are degenerate at $T = 4/3(\bar{J} + \Delta)$. The average jump in the internal energy Δe at this temperature can be estimated by the approximation
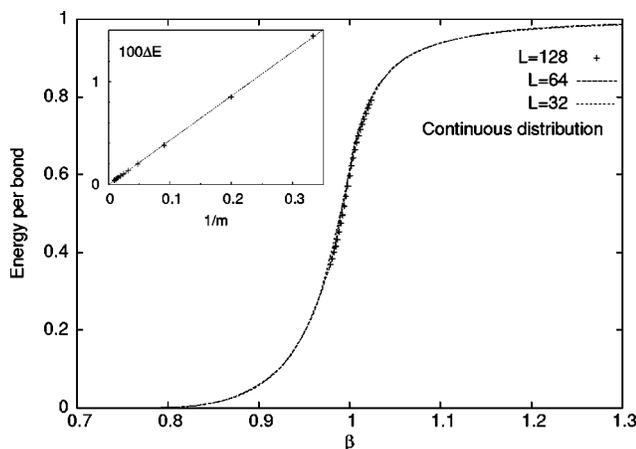

FIG. 6. Internal energy for (quasi)continuous disorder as given in Eq. (19). In the inset the latent heat is plotted as a function of the inverse number of the discrete peaks in the distribution.

with independent plaquettes, where a fraction of $1/8$ squares have the above degeneracy, each of which gives a local jump per site of $3T/4$. Thus $\Delta e \approx 3T/32$ which agrees reasonably well with the measured jump in Fig. 5.

The average internal energy displays also a finite jump at the transition point, as illustrated in the inset to Fig. 5. For the bimodal distribution this jump comes from those configurations in which a corner site has a strong and a weak bond, so that the isolated corner and the connected corner have the same contribution. The fraction of these corners is finite at the transition point, which leads to a finite average jump. Note, however, that the positions of these degenerate corners are distributed overall in the sample, thus their contribution is not exclusively related to the appearance of a percolating cluster.

The jumps in the average internal energy will disappear, if a continuous distribution of disorder is used. To illustrate it we used a distribution, which consists of $2m$ discrete peaks of equal weight:

$$P_m(J) = \frac{1}{2m} \sum_{k=0}^{m-1} \{\delta(\bar{J} - \Delta - [(m-1)/2 - k]\varepsilon - J) + \delta(\bar{J} + \Delta$$

$$+ [(m-1)/2 - k]\varepsilon - J)\} \quad (19)$$

so that in the large-m limit we approach a continuous distribution. In Eq. (19) ε is a small number, and in the simulation $\varepsilon = 2\bar{J}10^{-5}$ has been used. As shown in the inset to Fig. 6 the jump in the average internal energy at the transition point goes to zero as $\sim 1/m$, which can be understood as follows. For a given corner site out of m^2 different coupling sets there are only m for which the degeneracy, as described for the bimodal distribution, holds. Therefore the average jump should scale with $1/m$, as observed.

Going back to the internal energy for the bimodal distribution we argue that the true singularity can be observed at two sides of the transition point, i.e., as $t \to 0^+$ or $t \to 0^-$. In a finite system of length L, we expect a singularity in the form

$$e(t,L) = e(0^+, L) + t^{1-\alpha}\tilde{e}(tL^{1/\nu}), \quad t > 0, \quad (20)$$

and similarly for $t \leq 0$. Here the specific heat exponent α satisfies the hyperscaling relation: $d\nu = 2 - \alpha$. The scaling function $\tilde{e}(y)$ is expected to be an odd function and, thus, for small argument, to behave as $\tilde{e}(y) \sim y$. The scaling prediction in Eq. (20) has been checked and the results are shown in Fig. 7. The scaling collapse of the data is indeed very good with the exponents $\nu = 1$ and $\alpha = 0$, as conjectured in Eq. (9). From the collapse of the points we estimate $\nu = 1$ within a numerical precision of 1%.

As we mentioned below Eq. (18) one can define a transition temperature $T_c(L)$ in a given finite sample, which separates the regime in which there is a percolating cluster from that in which the largest cluster is not percolating. (We note that the percolating cluster at strong enough disorder, i.e., when $l_b \ll L$, is fractal, in contrary to the cluster at the breaking-up strength of disorder in Fig. 1, which is compact.) The distribution of this temperature for bimodal and continuous disorder is shown in Fig. 8 for periodic boundary conditions. For large systems one expects that the distribu-
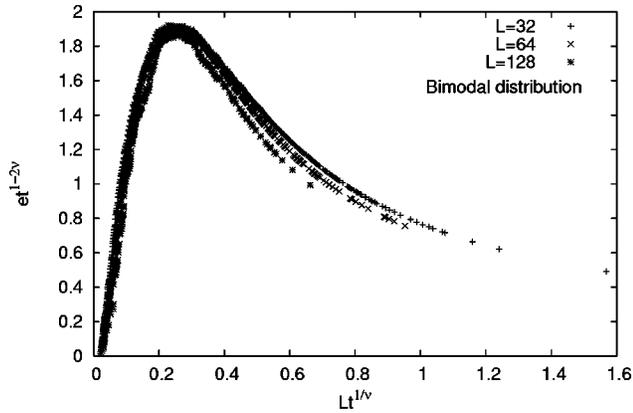
FIG. 7. Scaling plot of the singular part of the internal energy in Eq. (20) for bimodal disorder. In the plot there is one free parameter ν for which we used the conjectured value in Eq. (9).

tions approach a unique limiting curve in terms of the scaled variable $\tau = t_c/\sigma$, where $t_c = T_c(L) - T_c$ is the distance from the critical temperature in the infinite system and the variance of the distribution scales as $\sigma(L) \sim L^{-\omega}$, with some scaling exponent ω. As seen in Fig. 8 this limiting distribution, $P(\tau)$, has its maximum in $\tau > 0$ and the integrated distribution is $P_{sp} = \int_0^{-\infty} P(\tau) d\tau > 1/2$. As a matter of fact P_{sp} is the spanning probability given by the fraction of samples in which the largest cluster is percolating. Indeed a large (but finite) sample percolating at $\tau > 0$ is also percolating at $T = T_c$. According to our numerical results for the bimodal distribution $P_{sp} = 0.63(1)$. The finite-size corrections to the spanning probability are given by $P_{sp} - P_{sp}(L) \sim \Delta t(L)$, where $\Delta t(L) \sim L^{-\epsilon}$ is the shift of the critical temperature. Here we note
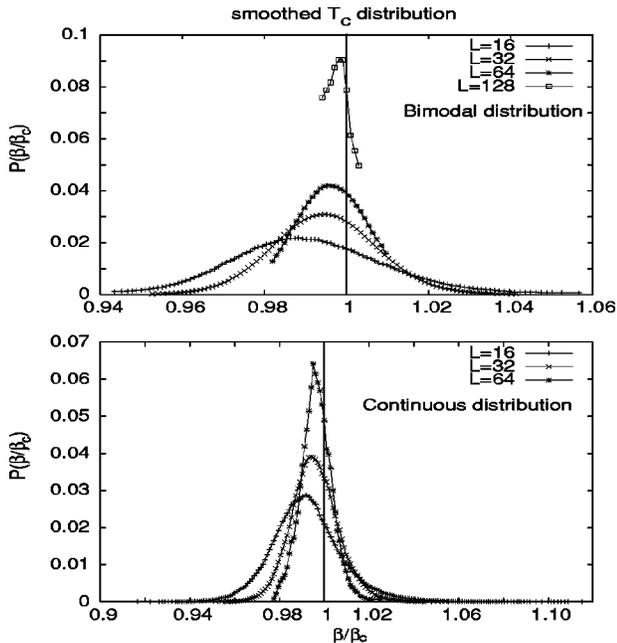

FIG. 8. Distribution of the finite-size (percolation) transition temperature for the bimodal (a) and the continuous (b) disorder for different sizes of the system. Note that the difference from the exact transition temperature is in the same order as the variance.
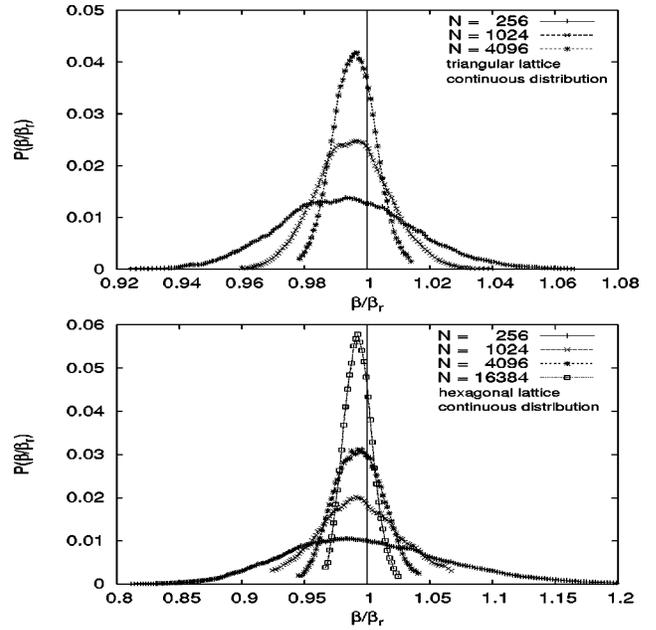

FIG. 9. Distribution of the finite-size transition (percolation) temperature for triangular and hexagonal lattices with continuous distribution of disorder for different sizes.

that in a pure system the shift exponent is generally given by $\epsilon = 1/\nu$, if the transition is of second order. If, however, the transition is of first order the critical exponent is given by its discontinuity fixed point value [23,24], which is $\nu_d = 1/d$. This is in accordance with the exact result in the pure model, in which the shift in the transition temperature is given by $\sim 1/N$, as given below Eq. (13). From the available data we could not make an independent estimate for ϵ^*; however, the data points seem to be consistent with $\epsilon = 1/\nu = 1$ for bimodal randomness. The exponent ω could be determined also with relatively large errors giving an estimate $\omega = 0.9(1)$.

We have also studied the location of the critical point on the triangular lattice, for which the coordination number is $z = 3$, and on the hexagonal lattice, which has $z = 3/2$. In Fig. 9 we present the distribution of the finite-size critical temperatures for different values of the number of sites N for the triangular and hexagonal lattices, with symmetric and continuous disorder, and for periodic boundary conditions. Here we take as reference temperature $\beta_r = 1/(z\bar{J})$, which is the transition point for the nonrandom system and expected to be a good approximation for symmetric disorder. The spanning probability at the reference temperature is $P_{sp} = 0.65(5)$ for both kinds of lattices, which is close to that in the square lattice.

V. MAGNETIZATION AND THE FRACTAL PROPERTIES OF THE PERCOLATING CLUSTER

Order and correlations in the RBPM are related to the structure of clusters in the optimal set G^*. As we explained in Sec. II at the critical point the largest cluster is a fractal, its mass M scales with the linear size of the system L as $M \sim L^{d_f}$. The structure of a typical optimal set is illustrated in
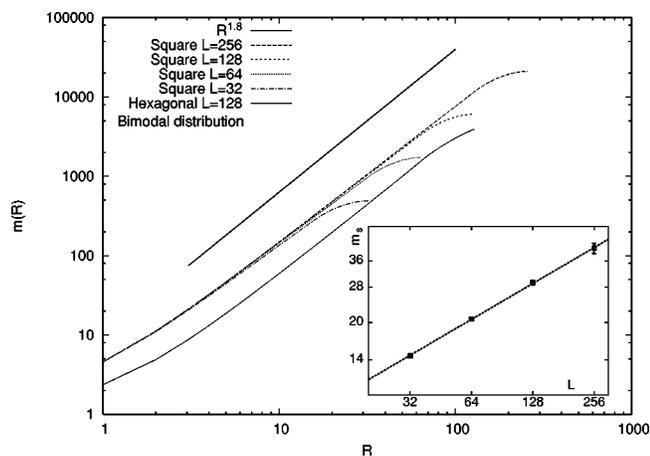
FIG. 10. Average mass of the percolating cluster within a region of size r at the critical point for the square and the hexagonal lattices. The conjectured asymptotic behavior is indicated by a straight line. Inset: average mass of surface points of the percolating cluster in the square lattice.
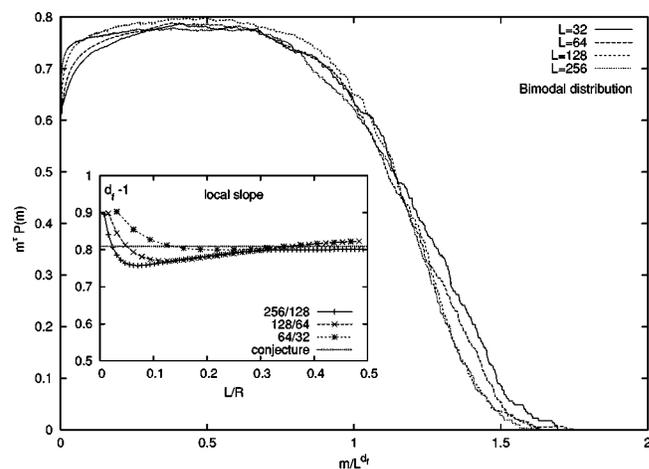

FIG. 11. Scaling plot of the cumulative distribution of the mass of the clusters at the critical point, using the conjectured value of the fractal dimension in Eq. (7). In the inset the fractal dimension is presented as calculated from the ratio of the masses of the percolating clusters in different finite systems (see text).

Fig. 1 of Ref. [16] for the bimodal distribution. Note that in G^* each connected component contains all the possible edges, since the inclusion of any coupling with $J_{ij} > 0$ will increase the cost function. The topology of clusters in ordinary bond percolating is evidently different, since they contain all the strong bonds but none of the weak ones.

We checked numerically that the largest cluster is indeed a fractal by measuring the number of points in the cluster, $\mu(r,L)$, which are at most at distance r from a reference point. Similarly we measured the number of points in the cluster in the distance between $r+1$ and r: $s(r,L) \equiv \mu(r+1,L) - \mu(r,L)$. Here we performed averaging (i) over the position of the reference point and (ii) over the disorder realizations. Under a scaling transformation, $r \to r/b$, $\mu(r,L)$ and $s(r,L)$ are expected to behave as

$$\mu(r,L) = b^{d_f}\mu(r/b,L/b),$$

$$s(r,L) = b^{d_f-1}s(r/b,L/b), \tag{21}$$

Now in the first equation taking $b=r$ we obtain $\mu(r,L) = r^{d_f}\tilde{\mu}(L/r)$, thus in a log-log plot one should obtain a straight line for $L > r$. As seen in Fig. 10 this relation is indeed satisfied both for the square and for the hexagonal lattices, in both cases—within the error of the calculation—having the same asymptotic slopes, which are compatible with the conjectured result in Eq. (7). We also performed a multifractal analysis showing only a single fractal dimension.

To have a more precise estimate of the fractal dimension we calculated $s(r,L)$ for finite systems of sizes $L = 16$, 32, 64, 128, and 256. Comparing results of two consecutive sites we obtained d_f from the second equation of Eq. (21) by setting $b=2$. The effective fractal dimensions as plotted in the inset to Fig. 11 have only weak r/L and L dependences, and from the asymptotic behavior one can estimate

$d_f = 1.81(1)$ in good agreement with the conjectured result in Eq. (7).

Next we studied the cumulative distribution of the mass of the clusters, $R(M,L)$, which measures the fraction of clusters having at least a mass of M. According to scaling theory [25] it should asymptotically behave as

$$R(M,L) = M^{-\tau}\tilde{R}(M/L^{d_f}) \tag{22}$$

with $\tau = (2-d_f)/d_f$. Note that the scaling relation in Eq. (22) contains only one free parameter d_f which can be estimated from an optimal scaling collapse of the distributions calculated for different sizes. As shown in Fig. 11 the scaling collapse is excellent if the conjectured fractal dimension in Eq. (7) is used. By analyzing the accuracy of the collapse we obtained an estimate, $d_f = 1.810(5)$, in very good agreement with the conjectured value.

We close this section by studying the surface magnetization of the model. Using open boundary conditions we measure the average mass of the surface sites belonging to the largest cluster, M_s. According to considerations in Sec. II in a finite system at the critical point this should asymptotically behave as $M_s \sim L^{d_f^s}$. According to the data presented in the inset to Fig. 10 the surface fractal dimension is given by $d_f^s = 0.495(10)$, which is in good agreement with the conjectured value in Eq. (8).

VI. ANISOTROPIC RANDOMNESS AND RELATION WITH THE STRONG DISORDER FIXED POINT OF RANDOM QUANTUM CHAINS

In this section the random bond Potts model is related to another problem of statistical physics, which has partially exact results about its critical properties. The analogies and relations between the models will be used to conjecture the values of the critical exponents in the random bond Potts model, which are already announced in Eqs. (7)–(9).

The problem we consider first is the Potts model with correlated bond disorder, in which the vertical bonds are constant denoted by $J_\parallel$, whereas the horizontal couplings have the same value in a given column, $i=1,2,\ldots,L$, denoted by J_i. Here the J_i are i.i.d. random variables and in the following we choose $J_\parallel = \bar{J}$. This model, which for Ising spins is the well-known McCoy-Wu model [3], is translationally symmetric in the vertical direction. Consequently the optimal set has a striplike structure, and the 2D diagram G is uniquely characterized by its 1D cut, denoted by g. The cost function of the problem can be written as $\phi(G) = L_\parallel \psi(g)$, where the size of the system in the vertical (horizontal) direction is $L_\parallel \sim L(L)$ and

$$\psi(g) = c_1(g) + \frac{1}{L_\parallel}c_2(g) + \beta \sum_{ij \in g} J_{ij} + \beta \bar{J}[L - c_1(g)] \quad (23)$$

is the cost function of the 1D problem. Here $c_1(g)$ is the number of isolated points and $c_2(g)$ is the number of connected diagrams which have at least two sites. In the thermodynamic limit the second term in the rhs is negligible and redefining the temperature we arrive to an equivalent cost function

$$\widetilde{\psi}(g) = c_1(g) + \widetilde{\beta} \sum_{ij \in g} J_{ij}, \quad (24)$$

with $\widetilde{\beta} = \beta/(1-\beta\bar{J})$ and at the critical point $\widetilde{\beta}\bar{J} = 1$. The optimization problem in Eq. (24) will be the subject of a separate publication.

Next we consider the extreme anisotropic [26] (time continuum or Hamiltonian) limit of the strip-random Potts model, where we let $J_\parallel/\bar{J} \to 0$ and the transfer matrix of the model in the vertical direction is written as $\mathcal{T} = \exp(-\tau \mathcal{H})$. Here τ is the (infinitesimal) lattice spacing and $\mathcal{H}$ is the Hamiltonian of a random Potts chain in the presence of a transverse field [24]:

$$\mathcal{H} = -\sum_i J_i \delta(s_i, s_{i+1}) - \sum_i \frac{h}{q}\sum_{k=1}^{q-1} M_i^k, \quad (25)$$

where $M_i|s_i\rangle = |s_i+1, \mathrm{mod}\ q\rangle$. If the couplings in vertical lines vary randomly from line to line then the transverse fields h_i are random variables, too. The fixed point of the 2D strip-random Potts model and that of the random quantum Potts chain with Hamiltonian in Eq. (25) are isomorph, thus they have the same set of critical exponents. The latter system has been studied in detail by a strong disorder renormalization group method, which was originally introduced by Ma, Dasgupta, and Hu [27] and used later by Fisher [17] and others [28–30]. This method is assumed to give asymptotically exact results; in particular the critical exponents for $q \geq 2$ are identical [28] and are given by [17]

$$\nu_\perp = 2, \quad x_\perp = 1 - \phi/2, \quad x_\perp^s = 1/2, \quad (26)$$

which also hold for the 2D strip-random model.

Having the critical behavior in the presence of correlated, anisotropic randomness we try to relate it to the original problem, in which the disorder is isotropic. To do so we imagine that at the fixed point of the anisotropic problem we let the couplings to be random also in the vertical direction. In this way translational symmetry in the vertical direction is broken and in the originally homogeneous strips connected and disconnected parts will appear. At the critical point these two (creation and destruction) processes are symmetric, therefore it is plausible to assume that the mass of the largest cluster stays invariant. Thus $M \sim L_\parallel \times L^{1-x_\perp} \sim L^{d_f}$, from which the value of the fractal dimension $d_f = 2 - x_\perp$ as announced in Eq. (7) follows. Repeating this argument for a surface cluster we obtain the result in Eq. (8). Another, and related, assumption is that the correlation volume, i.e., the surface of the largest cluster, grows in the same way in the two problems, as the transition point is approached. This means that $V(t) \sim \xi_\parallel(t)\xi_\perp(t) \sim L_\parallel |t|^{-\nu_\perp} \sim \xi(t)^2 \sim |t|^{-2\nu}$, from which $\nu = \nu_\perp/2 = 1$ follows, in accordance with the announced result in Eq. (9).

VII. CONCLUSION

One of the most spectacular effects of quenched disorder is the rounding of first-order transitions. In 2D this phenomenon cannot be studied in a perturbative basis around the pure systems' fixed point. In this paper we have demonstrated that an almost complete understanding of this phenomenon can be achieved in the other limiting case, when the effect of disorder is strong and dominates the critical behavior. We argued that the appropriate system for this purpose is the random bond ferromagnetic Potts model in the large-q limit, in which thermal fluctuations are strongly suppressed. In the random cluster representation the properties of the system are related to the dominant diagram of the high-temperature expansion. At the critical point this diagram is a self-similar fractal, giving a natural explanation of the diverging length scale, and its bulk and surface fractal dimensions are related to the critical exponents of the transition. We have introduced a plausible mapping between our isotropic system and that of strictly correlated disorder, which is isomorph with random quantum spin chains for which the critical properties are known. The critical properties conjectured in this way are then checked by large scale numerical calculations based on a very efficient combinatorial optimization algorithm. We have studied in detail the possible differences in the results obtained for discrete or continuous disorder. For discrete randomness, such as the bimodal one, which is frequently used in numerical calculations, the internal energy displays discontinuities, also the latent heat is finite. This observation should make people cautious while analyzing data obtained by the use of discrete disorder.

The results of this paper can be extended in several directions. Including in the distribution of the couplings the values $\beta J_{ij} < 0$ and $\beta J_{ij} > 1$ we obtain a system in which percolation and random bond effects compete. This problem can also be studied by our optimization algorithm and the properties of the stable fixed point can be calculated by analyzing the fractal properties of the relevant diagrams. Another extension is to include negative couplings, thus a Potts spin-glass problem is obtained. This still can be formulated as an
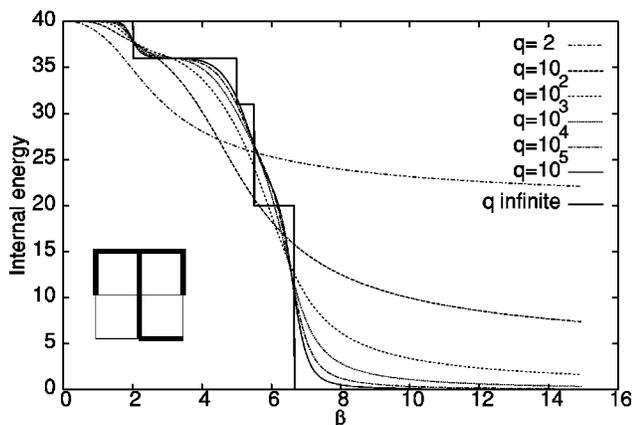
FIG. 12. Average internal energy as a function of β for various values of q. In the inset the analyzed plaquette is shown, where the thick lines represent strong bonds ($J=5$) and the thin lines weak ones ($J=1$).

optimization problem, which is most probably np-complete. Considering the ferromagnetic case one can try to perform a large-q expansion around the conjecturedly exact results. For the critical exponents the corrections are expected to go as $1/\ln q$ [15]. Finally, a further possible study is to clarify the dynamical properties of the system and to show if there are some relations with the ultraslow dynamics present in random quantum spin chains [17,31].

ACKNOWLEDGMENTS

APPENDIX

Here we present two examples to illustrate the discontinuous nature of the internal energy in the $q \rightarrow \infty$ limit.

We start with a 3×3 plaquette of the square lattice in which the couplings are 1 or 5 with the same probability. The realization we investigate is shown in the inset to Fig. 12. To illustrate the approach to $q \rightarrow \infty$ we have calculated for different values of q the internal energy as a function of the reduced temperature ($T \rightarrow T \ln q$), as introduced below Eq. (1). As seen in Fig. 12 for any finite q the internal energy is continuous and becomes discontinuous only in the $q \rightarrow \infty$ limit.

Our second example is to illustrate the effect of rounding due to averaging over disorder. We consider here an elementary triangle in which the edges carry the (positive) weights:

a, b, and c ($a = \beta J_a$, etc.). By simple inspection one finds that, for a given triplet $\{a,b,c\}$, the free energy is

$$-\beta F_{a,b,c}(\beta) = \begin{cases} 1 + \beta(\tilde{a} + \tilde{b} + \tilde{c}) & \text{if } \tilde{a} + \tilde{b} + \tilde{c} \leq \dfrac{2}{\beta} \\ 3 & \text{if } \dfrac{2}{\beta} \leq \tilde{a} + \tilde{b} + \tilde{c} \end{cases}$$

when $\tilde{a} + \tilde{b} \leq \tilde{c}$ and

$$-\beta F_{a,b,c}(\beta) = \begin{cases} 1 + \beta(\tilde{a} + \tilde{b} + \tilde{c}) & \text{if } \tilde{c} \leq \dfrac{1}{\beta} \\ 2 + \beta\tilde{c} & \text{if } \tilde{a} + \tilde{b} \leq \dfrac{1}{\beta} \leq \tilde{c} \\ 3 & \text{if } \dfrac{1}{\beta} \leq \tilde{a} + \tilde{b} \end{cases}$$

when $\tilde{c} \leq \tilde{a} + \tilde{b}$. We use the notation $\{\tilde{a}, \tilde{b}, \tilde{c}\} = \{a,b,c\}$ and $\tilde{a} \leq \tilde{b} \leq \tilde{c}$ (i.e., the variables with the tilde are ordered in ascending order).

For the uniform distribution of disorder in Eq. (12) with $\bar{J} = \Delta = 1/2$ one finds for the *average* internal energy

$$E(T) = \begin{cases} -\dfrac{1}{8}T^4 - T^3 + \dfrac{3}{2}, & T < 1 \\ -2T^4 + 8T^3 - 9T^2 + \dfrac{27}{8}, & 1 < T < \dfrac{3}{2} \\ 0, & \dfrac{3}{2} < T, \end{cases}$$

which is a continuous function of the temperature.

By contrast for the discrete bimodal distribution in Eq. (11) with $\bar{J} = 1/2$ and $\Delta = 1/\sqrt{3}$, which has the same mean and variance as the uniform distribution, the internal energy is given by

$$E(T) = \begin{cases} 0, & T < \dfrac{3}{4} - \dfrac{\sqrt{3}}{4} \\ \dfrac{3}{16} - \dfrac{\sqrt{3}}{16}, & \dfrac{3}{4} - \dfrac{\sqrt{3}}{4} < T < 1 - \dfrac{\sqrt{3}}{3} \\ \dfrac{3}{2}, & 1 - \dfrac{\sqrt{3}}{3} < T < \dfrac{1}{2} + \dfrac{\sqrt{3}}{6} \\ \dfrac{3}{4} - \dfrac{\sqrt{3}}{8}, & \dfrac{1}{2} + \dfrac{\sqrt{3}}{6} < T < \dfrac{3}{4} + \dfrac{\sqrt{3}}{12} \\ \dfrac{21}{16} - \dfrac{\sqrt{3}}{16}, & \dfrac{3}{4} + \dfrac{\sqrt{3}}{12} < T < \dfrac{3}{4} + \dfrac{\sqrt{3}}{12} \\ \dfrac{3}{2}, & \dfrac{3}{4} + \dfrac{\sqrt{3}}{12} < T. \end{cases}$$

This presents five discontinuities of width 0.079, 0.296, 0.158, 0.671, and 0.296 at the temperatures 0.317, 0.423, 0.789, 0.894, and 1.183, respectively.

[1] M. Aizenman and J. Wehr, Phys. Rev. Lett. **62**, 2503 (1989); **64**, 1311(E) (1990).

[2] Y. Imry and M. Wortis, Phys. Rev. B **19**, 3580 (1979); K. Hui and A. N. Berker, Phys. Rev. Lett. **62**, 2507 (1989).

[3] B. M. McCoy and T. T. Wu, Phys. Rev. **176**, 631 (1968); **188**, 982 (1969); B. M. McCoy *ibid.* **188**, 1014 (1969).

[4] For a review, see J. Cardy, Physica A **263**, 215 (1999).

[5] C. Chatelain, B. Berche, W. Janke, and P.-E. Berche, Phys. Rev. E **64**, 036120 (2001); W. Janke, P.-E. Berche, C. Chatelain, and B. Berche, e-print cond-mat/0304642.

[6] F. Y. Wu, Rev. Mod. Phys. **54**, 235 (1982).

[7] R. J. Baxter, J. Phys. C **6**, L445 (1973).

[8] M. Picco, Phys. Rev. Lett. **79**, 2998 (1997); C. Chatelain and B. Berche, *ibid.* **80**, 1670 (1998); Phys. Rev. E **58**, R6899 (1998); **60**, 3853 (1999); T. Olson and A. P. Young, Phys. Rev. B **60**, 3428 (1999).

[9] J. Cardy and J. L. Jacobsen, Phys. Rev. Lett. **79**, 4063 (1997); J. L. Jacobsen and J. Cardy, Nucl. Phys. B **515**, 701 (1998).

[10] S. Chen, A. M. Ferrenberg, and D. P. Landau, Phys. Rev. Lett. **69**, 1213 (1992); Phys. Rev. E **52**, 1377 (1995); S. Wiseman and E. Domany, *ibid.* **51**, 3074 (1995).

[11] J. T. Chayes *et al.*, Phys. Rev. Lett. **57**, 2999 (1986).

[12] P. W. Kasteleyn and C. M. Fortuin, J. Phys. Soc. Jpn. **26** (Suppl.) 11 (1969).

[13] R. Juhász, H. Rieger, and F. Iglói, Phys. Rev. E **64**, 056122 (2001).

[14] J.-Ch. Anglès d'Auriac *et al.*, J. Phys. A **35**, 6973 (2002).

[15] J. L. Jacobsen and M. Picco, Phys. Rev. E **61**, R13 (2000); M. Picco (unpublished).

[16] J.-Ch. Anglès d'Auriac and F. Iglói, Phys. Rev. Lett. **90**, 190601 (2003).

[17] D. S. Fisher, Phys. Rev. Lett. **69**, 534 (1992); Phys. Rev. B **51**, 6411 (1995).

[18] M. Grötschel, L. Lovász, and A. Schrijver, Combinatorica **1**, 169 (1981).

[19] W. Kinzel and E. Domany, Phys. Rev. B **23**, 3421 (1981).

[20] Similar arguments have been used for the 2D random field Ising model by T. Emig and Th. Nattermann, Eur. Phys. J. B **8**, 825 (1999); see also in Ref. [22].

[21] J. Galambos, *The Asymptotic Theory of Extreme Order Statistics* (Wiley, New York, 1978).

[22] E. T. Seppälä and M. J. Alava, Phys. Rev. E **63**, 066109 (2001).

[23] B. Nienhuis and N. Nauenberg, Phys. Rev. Lett. **35**, 477 (1975); M. E. Fisher and A. N. Berker, Phys. Rev. B **26**, 2507 (1982).

[24] L. Turban and F. Iglói, Phys. Rev. B **66**, 014440 (2002).

[25] See cf. in D. Stauffer and A. Aharony, *Introduction to Percolation Theory* (Taylor and Francis, London, 1992).

[26] J. Kogut, Rev. Mod. Phys. **51**, 659 (1979).

[27] S. K. Ma, C. Dasgupta, and C.-K. Hu, Phys. Rev. Lett. **43**, 1434 (1979); C. Dasgupta and S. K. Ma, Phys. Rev. B **22**, 1305 (1980).

[28] T. Senthil and S. N. Majumdar, Phys. Rev. Lett. **76**, 3001 (1996).

[29] F. Iglói, R. Juhász, and P. Lajkó, Phys. Rev. Lett. **86**, 1343 (2001).

[30] O. Motrunich *et al.*, Phys. Rev. B **61**, 1160 2000).

[31] F. Iglói and H. Rieger, Phys. Rev. B **57**, 11 404 (1998).